ELSEVIER

Sensors and Actuators A 97–98 (2002) 398–404

SENSORS AND ACTUATORS A PHYSICAL

www.elsevier.com/locate/sna

The application of nanosecond-pulsed laser welding technology in MEMS packaging with a shadow mask[☆]

Cheng Luo[*], Liwei Lin

Department of Mechanical Engineering, Berkeley Sensor and Actuator Center, University of California, Berkeley, CA 94720-1740, USA

Received 11 June 2001; received in revised form 27 November 2001; accepted 4 December 2001

Abstract

A nanosecond-pulsed laser bonding process with a shadow mask for MEMS packaging applications has been successfully demonstrated. YAG Surelit II laser with pulse duration of 4–6 ns, a wavelength of 355 nm and a focal diameter of 1 mm is used to provide the bonding energy for glass-to-silicon bonding using a 4 μm thick indium layer as the bonding material. The optimal bonding parameters are found experimentally when the laser energy is between 8 and 22 mJ and multiple laser shots are used. Furthermore, a regular white paper with pre-defined patterns has been successfully used as the masking material to achieve selective heating and bonding. Simulation results show that localized heating can be achieved by using the nanosecond laser. One micro-second after the laser power is applied, the temperature at the indium/silicon interface drops from 2500 to 760 °C and drops further to 43 °C after 1 ms. This nanosecond laser power is believed to provide suitable energy and time for localized heating and bonding applications for MEMS. © 2002 Elsevier Science B.V. All rights reserved.

Keywords: Laser; Bonding; Packaging; Mask; Heat transfer

1. Introduction

Various bonding approaches currently applied in MEMS packaging and fabrication have been reviewed in [1]. Previously, several bonding schemes based on localized heating and bonding have been proposed for MEMS packaging applications such as localized eutectic bonding [2], localized fusion bonding [3], localized solder bonding [4] and localized chemical vapor deposition (CVD) bonding [5]. However, the heating sources of these approaches are coming from resistive heating such that electrical wiring has to be provided. In many cases, the electrical wiring is not preferred.

A comprehensive review on laser welding was given in [6]. The laser welding represents a delicate balance between heating and cooling within a spatially localized volume overlapping two or more solids such that a liquid pool is formed and remains stable until solidification. The objective of laser welding is to create the liquid pool by absorption of incident radiation, allow it to grow to the desired size, and propagate this liquid pool through the solid interface eliminating the original seam between the components to be joined. The failure of welding is usually resulted due to too large or too small liquid pool or significant vaporization. The porosity and void formation during the welding process will affect the quality of the resulting weld. Basically, there are two types of laser welding: (a) conduction welding and (b) keyhole welding. The surface of the liquid pool in the former one remains unbroken, while it opens up to allow the laser beam to enter the liquid pool in the latter one.

Laser welding has advantages of high speed, high precision, consistent weld integrity, and low heat distortion. It is finding increasing use in industrial applications. Presently, people are focusing on welding metals (see, e.g., [7,8]), there has been little work done on laser welding of some important non-metal materials such as ceramics and glasses (see Chapter 6 of [6] for a simple review of laser welding of non-metals). Nd:YAG and CO_2 lasers are commonly used in industrial laser welding.

In the industrial laser welding, the size of two welded materials is usually large and heat-affected zone is generally not restricted. However, it is not so for laser bonding in MEMS packaging. The whole MEMS structure is small. The corresponding bonding area and heat-affected zone are highly restricted.

In the micro-scale, laser has been used to manufacture 3D microstructures [9], to assist alignment [10], and to perform inner lead bonding process [11]. However, little work has been presented on micro-scale laser sealing process for

[☆] A portion of this paper was presented in the Transducers '01/Eurosensors XV Conference at Munich, Germany, 10–14 June 2001.

[*] Corresponding author.
E-mail address: luo@me.berkeley.edu (C. Luo).

0924-4247/02/$ – see front matter © 2002 Elsevier Science B.V. All rights reserved.
PII: S0924-4247(01)00849-4

MEMS packaging applications. If successfully developed, laser welding could provide the advantages of no electrical wiring, fast operation and localized heating.

2. Experimental set up and bonding mechanisms

The laser bonding in our experiments belongs to the type of conduction welding with the surface of the liquid pool remaining unbroken. An Nd:YAG Surelit II laser with a pulse duration of 4–6 ns and a wavelength of 355 nm is used for glass-to-silicon bonding with an intermediate layer of indium. The experimental set up is shown in Fig. 1. A 4 μm thick indium layer is deposited on a 500 μm thick silicon wafer and a 500 μm thick Pyrex glass substrate is placed on top of the indium/silicon substrate. A certain pressure is applied in order to bring the glass and silicon wafers in close proximity. A mask consisting of reflective material is used to define the bonding area. In the first try-out experiment, a plain white paper with pre-defined open areas is used as the mask. The glass layer is virtually transparent to laser light with the wavelength of 355 nm, while the indium layer absorbs laser irradiation energy. The material at the places corresponding to the designated bonding area is removed from the mask such that laser light can pass through the glass and be absorbed by the bonding material. On the other hand, a reflective masking material serves as a good mask to prevent laser light penetration. Bonding material (indium in the current setup) in the spot of the laser irradiation forms a good bond with glass at elevated temperature. Experimentally, multiple laser shots at one spot allow more materials to react and provide more reaction time, which lead to stronger bonding results.

3. Mathematical models and simulation results

Different from that in the traditional macro-scale packaging applications, it is desirable to limit the heating area in the MEMS bonding process to avoid damages to devices outside the bonding area. The scheme of nanosecond laser bonding provides a unique approach to achieve localized heating and both mathematical model and simulation are essential to help determine the optimized heating power and time to achieve localized heating and bonding.

The heat conduction process between two contacting layers during and after laser irradiation has been discussed by various papers. For example, Grigoropoulos [12] considered the case that laser energy was absorbed by the top of the cap layer, and then passed to the whole cap and substrate layers. In addition, Gupta et al. [13] set up a one-dimensional model to consider the heat transfer in the two layers along the direction perpendicular to the layers after the interface absorbed laser energy. They assumed that the laser heating is a surface input directly on the interface. In this work, our experimental set up is similar to that of [13]. However, we need to determine the temperature distribution along the direction parallel to the layers as well as that perpendicular to the layers. In addition, we consider the laser irradiation as a volumetric heating source. Therefore, we establish a two-dimensional model with laser energy as a volumetric input.

Laser heating of metals involves two major microscopic energy deposition processes: absorption of radiation energy by free electrons and subsequent heating of the metal lattice through electron–lattice collisions. It has been characterized that the absorption depth from a nanosecond laser to indium is in the order of micro-meter [14] and a volumetric heating source is assumed. While non-Fourier heat conduction model is suggested for laser heating process of metals with a pulse duration of femtoseconds, the conventional Fourier one is good enough to model heating of metals with a nanosecond-pulsed laser [15]. Therefore, in this work, we set up our mathematical models based on the Fourier heat conduction equations. The incident laser power intensity distribution is considered as Gaussian

$$I(r,z,t) = (1-R)\frac{2P}{\pi\omega^2}\exp\left(-\frac{2r^2}{\omega^2}\right)\exp(-az)^* H(t), \qquad (1)$$

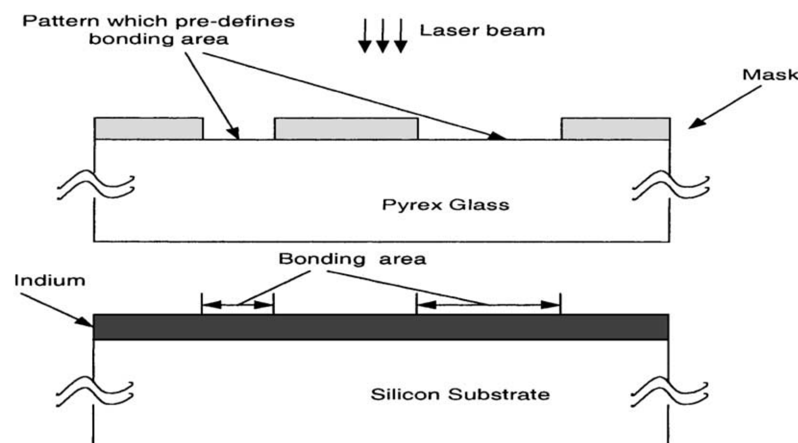

Fig. 1. The experimental set up of glass-to-silicon bonding with an intermediate layer of indium and a built-in mask.

where R is the reflectivity, P the laser output power and ω the radius of the incident laser beam. z represents the coordinate along vertical direction, r stands for the coordinate along horizontal direction, t denotes time, a stands for laser light absorption coefficient, $z = 0$ at the interface of indium and glass, $r = 0$ in the center of laser beam, and $H(t)$ represents the time variation of the pulse and has the form of a unit step input:

$$H(t) = \begin{cases} 1 & \text{as } 1 < t < t_{\mathrm{p}}, \\ 0 & \text{as } t > t_{\mathrm{p}}. \end{cases} \tag{2}$$

The governing equation in the indium layer during the pulse duration is

$$\rho C \frac{\partial T}{\partial \tau} = k\left[\frac{\partial^2 T}{\partial r^2} + \frac{1}{r}\frac{\partial T}{\partial r} + \frac{\partial^2 T}{\partial z^2} + I(r,z,t)\right], \tag{3}$$

where ρ denotes mass density, C the specific heat, T stands for temperature, k denotes heat conduction coefficient, and ρ, C and k will change with temperature.

Pyrex glass is virtually transparent to the laser beam with a wavelength of 355 nm. Also, in our experiments, there is no visible damage on the glass after laser irradiation of such a wavelength. Therefore, the absorption of laser irradiation in the glass layer is negligible. The governing equations in the glass and silicon are the same during the pulse duration and of the form:

$$\rho C \frac{\partial T}{\partial \tau} = k\left[\frac{\partial^2 T}{\partial r^2} + \frac{1}{r}\frac{\partial T}{\partial r} + \frac{\partial^2 T}{\partial z^2}\right]. \tag{4}$$

The boundary conditions during the pulse duration at the interface of indium and glass and that of indium and silicon are the same and of the form

$$\left(k\frac{\partial T}{\partial x}\right)_{\text{glass}} = \left(k\frac{\partial T}{\partial x}\right)_{\text{substrate}}. \tag{5}$$

At $t = 0$, the temperature of the whole structure is uniform and is equal to the ambient temperature, 300 K.

$$T(r,z,t=0) = 300\,\mathrm{K}. \tag{6}$$

It is assumed that there is no heat loss at the upper surface of glass layer and lower surface of silicon layer by radiation, convection, and conduction.

$$\frac{\partial T}{\partial z} = 0. \tag{7}$$

At the center, because of the axisymmetry of temperature distribution;

$$\frac{\partial T}{\partial r} = 0. \tag{8}$$

At the place, the temperature is the same as the ambient temperature, 300 K, i.e.

$$T(r \to \infty, z, t) = 300\,\mathrm{K}. \tag{9}$$

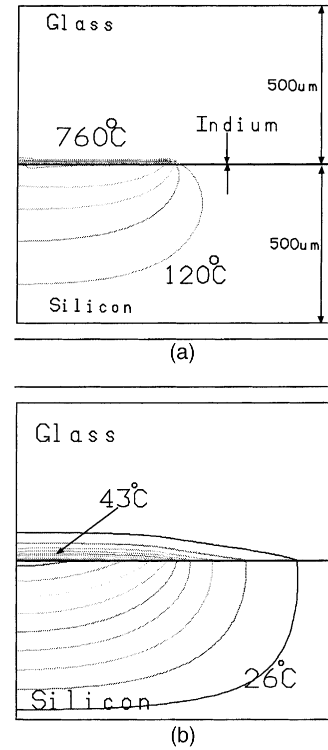

Fig. 2. Two simulation results of isotherms on the cross-section: (a) the result after 1 μs; (b) the result after 1 ms.

After the pulse duration, the governing equations in each layer are the same and of the form

$$\rho C \frac{\partial T}{\partial \tau} = k\left[\frac{\partial^2 T}{\partial r^2} + \frac{1}{r}\frac{\partial T}{\partial r} + \frac{\partial^2 T}{\partial z^2}\right]. \tag{10}$$

In this case, the boundary conditions (5) and (7)–(9) are still valid, while Eq. (6) cannot be used as the initial condition. The initial temperature distribution in this case is the one just after one pulse duration.

As shown in Fig. 2, two simulations using software ANSYS 5.5 have been conducted to examine heating zones on the cross-section after 1 μs and 1 ms after the indium layer absorbs energy, respectively. The laser beam is 1 mm in diameter in this case, and the energy is 22 mJ. This energy of 22 mJ is the maximum energy found to achieve a good bond in our experiments (see Fig. 3), which will be given in details in the next section. Due to symmetry of the problem, only half of the domain is simulated. It is estimated that the initial temperature at the bonding interface can be as high as 2500 °C after the nanosecond laser is applied. The heat conduction occurs rapidly such that highest temperature decreases to 760 °C in 1 μs and 43 °C in 1 ms. Previously, it has been demonstrated that rapid thermal processing is capable of creating hermetic bonding with a temperature at 990 °C for 2 s for the aluminum–nitride bonding system [16]. It appears from this numerical simulation that the high temperature zone of more than 760 °C can last less than 1 μs in the bonding process. Therefore, the processing time may not be enough for diffusion bonding as suggested in [16]. On

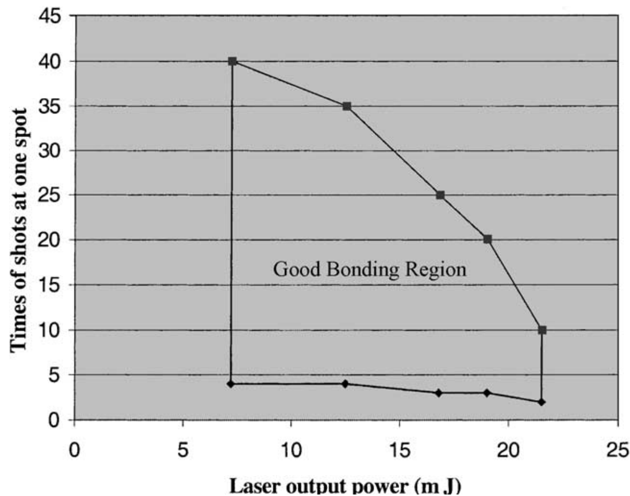

Fig. 3. A good bonding region used to choose laser output energy and shots at one spot with other parameters fixed.

the other hand, the temperature distribution drops dramatically after only 1 μs as seen in the simulation result such that the heat-affected zone is very limited in this case.

4. Experimental results

To examine the applicability of nanosecond laser bonding, experimental work on good bonding region, bonding strength, and masking materials have been investigated. Since the laser power density has a Gaussian distribution, the bonding area is expected to be a circular shape on the bonding plane and the bonding diameter depends on the applied laser energy and duration of the laser shots. Different levels of laser energy and shots have been investigated to determine the optimal bonding conditions. Several observations are concluded. (1) Laser output energy higher than 22 mJ damages the bonding interface and leads to the failure of bonding. It is believed that the failure is due to significant vaporization. (2) Laser output energy lower than 7 mJ fails to generate enough energy to form a strong bond. In our understanding, it is due to that the liquid pool is too small. (3) A single shot at one spot normally does not form a good bond. It is believed that the high power nanosecond laser creates a shock wave in the interface and that may significantly degrade the intimate contact and cause bonding failure. After the first shot, the melted indium forms uneven surface at the interface and those peak areas may achieve intimate contact with the top glass wafer and become bonding sites in the subsequent laser bonding shots. (4) Too many shots at one spot may destroy the bond which has already been formed previously. For example, over 40 shots with the laser output energy of 7 mJ and over eight shots with the laser output energy of 22 mJ get poor bonding results. Experimental results show that high energy laser together with multiple shots may severely damage the bonding surface to a certain degree such that the uneven surface fail to produce enough contact areas for good bonds. Therefore, they are characterized as bonding failures. If the bonding strength is comparable to the yielding strength of indium of 2.6 MPa (note that Pyrex glass is stronger than indium), then we define the bond as a good one. Based on the general observations and the definition of a good bond, a successfully bonding region is drawn with respect to the laser output energy and shots as shown in Fig. 3.

The typical bonding result is shown in the optical photograph of Fig. 4(a) that is taken after laser output energy of 10 mJ of 1 mm in diameter for 10 shots. In this case, glass-to-indium bond is forcefully broken in order to examine the bonding interface. The dark color on the silicon substrate is believed to be the residuals of indium after high-energy laser is applied. The SEM pictures shown in Fig. 4(b) and (c) are taken from the glass and silicon substrates, respectively, at the bonding interface. It can be seen that part of the indium layer is attached to the glass substrate. It is believed some of the indium residuals may be coming off the silicon substrate due to evaporation. However, a flat ring shape boundary can be identified in Fig. 4(c) and it seems to represent intimate contact with the top glass wafer and is being separated under the external force. Therefore, it is believed that the bonding strength as these areas may be comparable to the yielding strength of indium of 2.6 MPa.

After the nanosecond laser bonding experiments are investigated, masking materials are studied, which are used to protect devices outside the bonding area. In laser manufacturing, several methods have been adopted to reduce the loss of laser energy due to reflectivity on the surface of target metal [17].

1. A thin film of metal of relatively lower reflectivity is put on the layer of target metal to absorb laser irradiation. The introduced metal is required to be able to form alloy with target metal.
2. It is well known that black color is of the highest absorption rate to a visible laser light. A thin film of the color of black is deposited on the layer of target metal using chemical or physical treatment to absorb relatively more laser irradiation. This is so-called blackening treatment.
3. The reflectivity of target metal might increase with the decrease of laser incident angle.
4. The absorbed laser irradiation will increase together with the surface roughness of target metal.

However, in our case, it is expected that most of laser irradiation outside the pattern is reflected by the masking material and that pattern on the mask remains unchanged during the bonding process. Based on these, there are two basic requirements for a good reflective masking material. (1) At best only a small amount of the material is molten after the laser irradiation. Otherwise, the pattern on the material to pre-define the bonding shape will be destroyed. (2) To avoid damage to the devices outside the bonding area, laser light is not allowed to go through the material in the places outside the pattern.

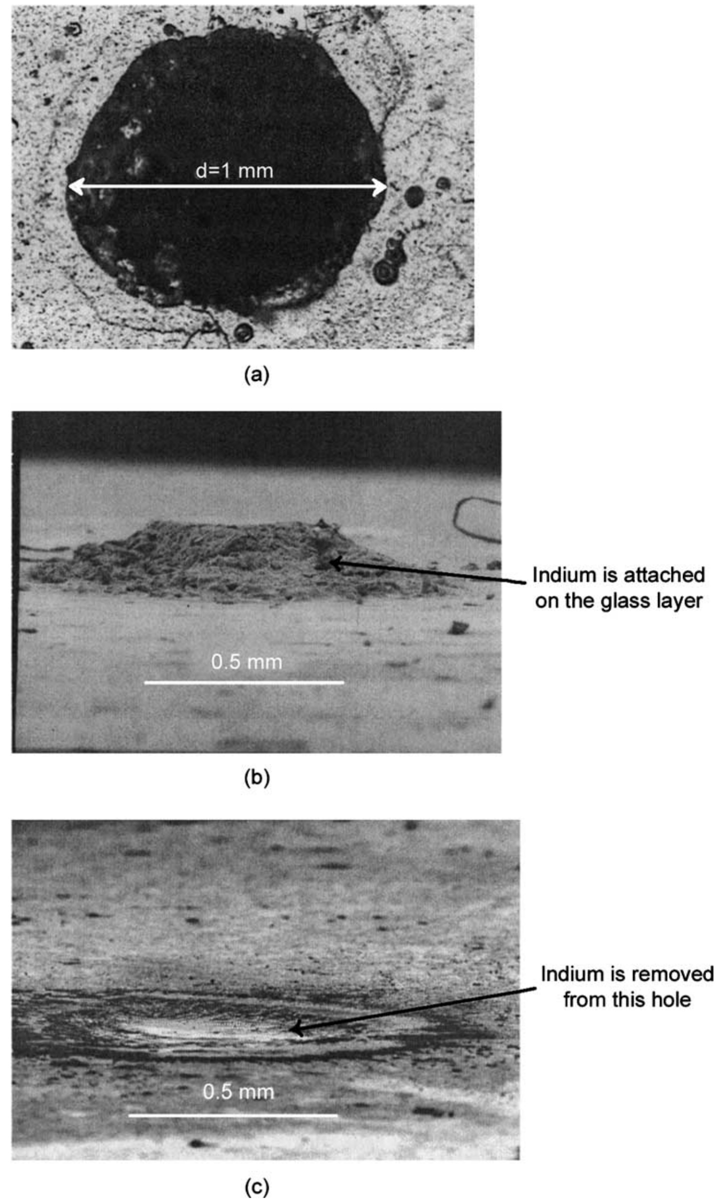

Fig. 4. A bonding result: (a) a top view (optical photo) of glass-to-indium bonding spot; (b) a cross-sectional view (SEM) of the bonding spot on the glass layer after the glass-to-indium bond is forcefully broken; (c) a cross-sectional view (SEM) of the bonding spot on silicon substrate.

The above methods in the laser manufacture aim to increase the target metal's absorption of laser irradiation, while the purpose in our case is to reduce the effect of laser irradiation on the masking material. We can use the ideas opposite to those adopted in the above methods in the laser manufacture to meet the two requirements for a good masking material. With this in mind, we have proposed five principles in choosing a reflective masking material. (1) Most of the laser lights should be reflected by the material. According to this, the color of the material is recommended to be white. The reason is that in principle all visible laser lights can be reflected by the material with the white color. (2) The higher the melting temperature of the material is, the better it is. A small portion of laser irradiation may be absorbed by the material. Consequently, the material of the relatively low melting temperature might be molten, while the material of the relatively high melting temperature might not. (3) Decrease the surface roughness as much as possible so that the absorbed laser irradiation will be decreased. (4) Control the incident angle of laser light to be 0°, i.e. the laser beam is irradiated perpendicular to the surface of target metal. (5) The mask material should have a certain thickness such that the pattern on a mask material could still be maintained even if the top part of mask material suffers small damage due to laser irradiation.

During our experiments, it is found that a plain white paper can serve as a good masking material to the YAG laser of the parameters indicated at the beginning of this paper. Our pattern generation on the paper is as follows: first print the desired pattern on the paper using a printer, and then cut

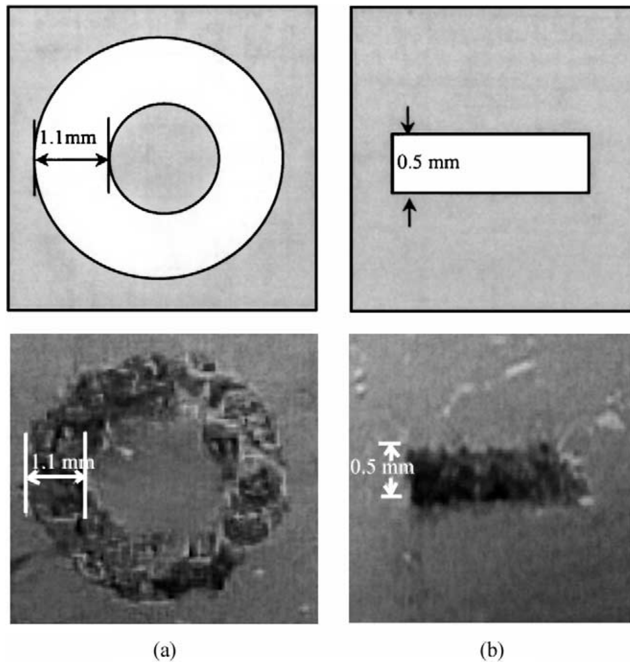

Fig. 5. A top view of two bonding results using a shadow mask after random shots by laser beam of 1 mm in diameter on the mask: (a) a ring-shape pattern on the mask and the corresponding bonding result; (b) a rectangular pattern on the mask and the corresponding bonding result.

the pattern using a commercial carving knife under a microscope. In such a way, the error in a pattern size is 50 μm. A way with a better control of the pattern size needs to be explored. In Fig. 5, two results are shown, respectively, corresponding to different patterns on plain white paper masks. The first one is a ring-shape pattern on the mask with a characteristic length of 1.1 mm, and the second one is a rectangular pattern on the mask with a characteristic length of 0.5 mm. As shown in Fig. 5, corresponding to different patterns on plain white paper masks, the laser light does not go beyond the pre-defined bonding area. Therefore, laser beam sizes can be larger or smaller than characteristic length of bonding area. This provides various options to choose laser beam sizes in the bonding process.

5. Conclusions

Based on the results described above, this approach has potential applications in MEMS packaging process. In the near future, we will focus on two issues to improve our approach. The first one is to explore more mask materials, and the second one is to investigate the exact mechanisms of indium–glass bond.

Acknowledgements

The nanosecond laser welding experiments are conducted in the NSF nanosecond laser facility in the Mechanical Engineering Department, University of California at Berkeley. The authors would like to thank Prof. C.P. Grigoropoulos for assistance of nanosecond laser and Mr. M. Chiao for providing samples and helping with simulation. They also want to thank an anonymous reviewer of this paper for very helpful comments. This work is supported in part by an NSF CAREER award (ECS 0096098) and a grant from DARPA MTO/MEMS program (F30602-98-2-0227).

References

[1] L. Lin, MEMS post-packaging by localized heating and bonding, IEEE Trans. Adv. Pack. 23 (2000) 608–616.
[2] L. Lin, Y.T. Cheng, K. Najafi, Formation of silicon–gold eutectic bond using localized heating method, Jpn. J. Appl. Phys., Part II 11B (1998) 1412–1414.
[3] Y.T. Cheng, L. Lin, K. Najafi, Localized silicon fusion and eutectic Bonding for MEMS fabrication and packaging, IEEE/ASME J. Microelectromechanical Syst. 9 (2000) 3–8.
[4] Y.T. Cheng, W.T. Hsu, L. Lin, C.T. Nguyen, K. Najafi, Vacuum packaging technology using localized aluminum/silicon-to-glass bonding, in: Proceedings of the IEEE Micro-Electro Mechanical Systems Conference, Interlaken, Switzerland, January 2001, pp. 18–21.
[5] G.H. He, L. Lin, Y.T. Cheng, Localized CVD bonding for MEMS packaging, in: Proceedings of the 10th International Conference on Solid-State Sensors and Actuators, Transducers'99, Technical Digest, Sendai, Japan, June 1999, pp. 1312–1315.
[6] W.W. Duley, Laser Welding, Wiley, New York, 1999, pp. 1–9.
[7] B. Irving, High-speed laser welds miles-long runs of thin wall stainless steel tubing, Weld. J. 77 (5) (1998) 28–30.
[8] W. Waddell, F.M. Davies, Laser welded tailored blanks in the automotive industry, Weld. Met. Fabric. 104 (1995).
[9] T.M. Bloomstein, D.J. Ehrlich, Laser deposition and etching of three-dimensional microstructures, in: Proceedings of the International Conference on Solid-State Sensors and Actuators, San Francisco, USA, 1991, pp. 507–511.
[10] J. Brown, N. Maier, K.Y. Lee, L. Ziegltrum, J.S. Leger, Laser Welding: providing alignment precision and accuracy to substrate level packaging, in: Proceedings of the International Society for Optical Engineering (SPIE), Vol. 3874, 1999, pp. 158–164.
[11] J.D. Hayward, Optimization and reliability evaluation of a laser inner lead bonding process, IEEE Trans. Compon. Pack. Manuf. Technol., Part B 17 (4) (1994) 547–553.
[12] C.P. Grigoropoulos, Heat transfer in laser processing of thin films, in: C.-L. Tien (Ed.), Annual Review of Heat Transfer, Vol. V, CRC Press, Boca Raton, FL, 1994, pp. 77–130.
[13] V. Gupta, A.S. Argon, D.M. Parks, J.A. Cornie, Measurement of interface strength by a laser spallation technique, J. Mech. Phys. Solids 40 (1) (1992) 141–180.
[14] X. Xu, C.P. Grigoropoulos, R.E. Russo, Transient temperature during pulsed excimer laser heating of thin polysilicon films obtained by optical reflectivity measurement, J. Heat Transf. 117 (1995) 17–24.
[15] T.Q. Qiu, C.L. Tien, Short-pulse laser heating on metals, Int. J. Heat Mass Transf. 35 (1992) 719–726.
[16] M. Chiao, L. Lin, Hermetic wafer bonding based on rapid thermal processing, in: Proceedings of the Technical Digest of Solid-State Sensors and Actuators Workshop, Hilton Head Island, June 2000, pp. 347–350.
[17] M. Cao, Q. Zheng, Z. Chen, Z. Chen, Laser Manufacturing, Central China University of Science and Technology Press, Wuhan, China, 1995, pp. 103–105, 327–330 (in Chinese).

Biographies

Cheng Luo received his BS degree in July 1993 in Engineering Mechanics from the Hunan University in China, his MS degree in May 1997 in Mechanical Engineering from the University of Houston, and his PhD degree in May 2000 in Mechanical Engineering from the University of California at Berkeley. He was a Master Student in the Department of Mechanics and Engineering Science at Beijing University in China from September 1993 to April 1995. He worked as a Structural Engineer in the Structural Department of National Oilwell Company in Houston from June 1997 to January 1998. He is presently a Research Fellow in Electronics Research Laboratory at the University of California at Berkeley. His research interests lie in the areas of MEMS packaging and fabrication, continuum and micro-mechanics, continuum and micro-heat transfer, and laser applications.

Liwei Lin received the MS and PhD degrees in Mechanical Engineering from the University of California at Berkeley in 1991 and 1993, respectively. He worked on the research and development of microsensors at BEI Electronics Inc., USA, from 1993 to 1994. From 1994 to 1996, he was an Associate Professor at the Institute of Applied Mechanics, National Taiwan University, Taiwan. From 1996 to 1999, he was an Assistant Professor at the Mechanical Engineering and Applied Mechanics Department at the University of Michigan, Anne Arbor. He joined the University of California at Berkeley in 1999 and is now an Associate Professor at Mechanical Engineering Department and Co-Director at Berkeley Sensor and Actuator Center, NSF/Industry/University Research Cooperative Center. His research interests are in design, modeling and fabrication of microstructures, microsensors and microactuators as well as mechanical issues in microelectromechanical systems including heat transfer, solid/fluid mechanics and dynamics. Dr. Lin is the recipient of the 1998 NSF CAREER Award for research in MEMS packaging and the 2000 ASME Journal of Heat Transfer Best Paper Award for his work on micro-scale bubble deformation. He led the effort in establishing the MEMS sub-division in ASME and is currently serving as the Vice-Chairman of the Executive Committee for the MEMS sub-division. He holds seven US patents in the area of MEMS.